Supporting Information

CFTR transmembrane segments are impaired in their conformational adaptability by a pathogenic loop mutation and dynamically stabilized by Lumacaftor

Georg Krainer,[1,#,§,*] Mathias Schenkel,[1,§] Andreas Hartmann,[1] Dorna Ravamehr-Lake,[2] Charles M. Deber,[2,*] Michael Schlierf[1,3,*]

From [1]B CUBE – Center for Molecular Bioengineering, Technische Universität Dresden, Tatzberg 41, 01307 Dresden, Germany; [2]Division of Molecular Medicine, Research Institute, Hospital for Sick Children, 686 Bay Street, Toronto, ON M5G 0A4; and Department of Biochemistry, University of Toronto, Toronto, ON M5S 1A8, Canada; [3]Cluster of Excellence Physics of Life, TU Dresden, 01062 Dresden, Germany.

Running title: *Effects of a CFTR loop mutation*

[#]Present address: Department of Chemistry, University of Cambridge, Lensfield Road, Cambridge CB2 1EW, United Kingdom

[§]Authors contributed equally to this work.

*To whom correspondence should be addressed: Georg Krainer (gk422@ch.cam.ac.uk), Charles M. Deber (deber@sickkids.ca), Michael Schlierf: B CUBE – Center for Molecular Bioengineering, Technische Universität Dresden, Tatzberg 41, 01307 Dresden, Germany; michael.schlierf@tu-dresden.de; Tel. +49 (0)351 463 43050.

Keywords: Cystic fibrosis transmembrane conductance regulator (CFTR), cystic fibrosis, single-molecule biophysics, membrane protein, helical packing, protein misfolding, pharmacological corrector, Lumacaftor, single-molecule fluorescence resonance energy transfer (FRET)

EXPERIMENTAL PROCEDURES

Materials and sample preparation. All reagents and chemicals were purchased with the highest purity available. Lipids (DLPC, 12:0 PC; POPC, 16:0–18:1 PC; DEiPC, 20:1 PC) were obtained from Avanti Polar Lipids, USA. Lumacaftor (VX-809) was obtained from Selleck Chemicals LLC, USA with a purity of 99.07% (Batch No. S156502). Dipicolinic acid (DPA) and $TbCl_3$ were purchased from Sigma-Aldrich, USA. CFTR E217G and WT TM3/4 hairpin variants for site-specific double labeling were constructed with two Cys residues placed at the N- and C-terminal ends of the CFTR sequence. Details on hairpin design can be found in Fig. S2. Hairpins were produced, purified, and labeled with FRET donor (ATTO532; Atto-Tec, Germany) and acceptor (ATTO647N; Atto-Tec) fluorophores as previously described (1). Purification was monitored by SDS-PAGE (Fig. S3). Hairpins were reconstituted into large unilamellar phospholipid vesicles (LUVs) to yield proteoliposomes with a protein-to-vesicle molar ratio of 1:10 (i.e., less than every tenth LUV contained one hairpin molecule). LUVs were prepared following standard procedures and reconstitution was performed as previously described (1). Formation of LUVs was confirmed by dynamic light scattering (DLS) (Malvern Zetasizer Nano S, Malvern, UK), yielding LUVs with a unimodal vesicle size distribution around a mean hydrodynamic diameter of ~120 nm.

Single-molecule FRET experiments. Measurements were carried out using a confocal fluorescence spectroscopy setup as previously described (1, 2). Unless stated otherwise, experiments were performed at 24°C in buffer (50 mM Tris, pH 7.4) on freely diffusing proteoliposomes at an effective hairpin concentration of <100 pM. For measurements at 37°C, the temperature in the sample chamber was adjusted and maintained by using an objective collar linked to a refrigerated circulator (F25-MC, Julabo, Germany). For measurements with Lumacaftor, sample solutions were supplemented with corrector at a concentration of 1 mM, diluted from a 100 mM stock solution in dimethyl sulfoxide. Samples were incubated for 24 h prior to measurements. Data analysis of single-molecule measurements was performed with custom-written Matlab scripts (Mathworks, USA) following procedures described previously (1). Briefly, bursts were identified with a burst search algorithm using a maximum interphoton time of 30 μs, a minimum total number of 100 photons after background correction, and a Lee filter of 4. FRET efficiencies were calculated from bursts exhibiting a stoichiometry ratio of $S = 0.2-0.7$ and an alternating laser excitation−two-channel kernel-based density distribution estimator (ALEX-2CDE) score smaller than 7. Additionally, bursts were rejected if the number of acceptor photons was less than 15 after donor excitation and more than 300 after acceptor excitation; these restrictions suppressed fluorescence background caused by impurities, multiple-molecule events or non-reconstituted protein aggregates. In measurements with Lumacaftor, bursts were regarded as significant if the minimum number of acceptor photons after acceptor excitation exceeded 40 and the total number of photons after donor excitation exceeded 50. A Lee filter of 10 was applied and a small acceptor subpopulation that was quenched was filtered out by selecting only bursts with an acceptor lifetime of $2 < \tau_A$. From all remaining bursts, FRET efficiency histograms were constructed with bin widths of 0.033. E values were corrected for background, direct acceptor excitation, channel cross-talk, as well as differences in detector efficiencies and quantum yields between the dyes, as described previously (1, 3). For PDA, apparent FRET efficiencies, E^*, were used by calculating FRET efficiencies without applying the aforementioned corrections. Plots of relative donor fluorescence lifetime versus FRET efficiency were created as previously described (1, 3, 4).

PDA fitting of FRET efficiency histograms was performed by using a static two-state PDA model (1, 4) to describe the equilibrium between the extended, open (O) and compact, folded (C) hairpin conformations with state fractions f_O and $f_C = 1-f_O$ as well as mean FRET efficiencies $E_C^*$and E_O^*, respectively. The model also included Gaussian distance distributions for folded and open states to account for additional widths ($\sigma_{C,O}$) in excess of shot-noise broadening. A Monte Carlo sampling-based regression algorithm in Matlab was employed to iteratively fit the experimental FRET efficiency histogram with the theoretical two-state static PDA histogram by chi-square minimization to optimize the fit parameters {f_C, σ_C, f_O, E_C^*, E_O^* }. An oversampling factor of 10 was used to gain sufficient statistics. The experimental FRET efficiency histogram employed in PDA fitting was created by selecting single time-bin segments of equal duration (i.e., T_b = 1 ms) from the center of each fluorescent burst and calculating the apparent FRET efficiency, E^*, for each bin.

Tb^{3+}/dipicolinic acid (DPA) fluorescence assay. To probe Lumacaftor membrane effects, we adapted a fluorescence-based leakage assay that involves the detection of fluorescence generated on the interaction of Tb^{3+} with DPA. In this assay, $TbCl_3$-loaded liposomes suspended in a solution containing DPA are treated with increasing concentrations of Lumacaftor. Any disturbance to the phospholipid bilayer, introduced by Lumacaftor, would result in the escape of terbium(III) (Tb^{3+}) ions from the liposomes. The interaction of DPA with Tb^{3+} causes fluorescence emissions that are 10,000 times higher than those of Tb^{3+} alone, thus enabling a sensitive readout of aqueous content leakage from Lumacaftor-treated vesicles.

To perform the assay using POPC lipid vesicles, 1 mL stock of POPC (equivalent to 25 mg) was dried into thin films, lyophilized, and brought up in 1 mL of water, vortexed, frozen on dry ice, and lyophilized again overnight. The resulting lyophilized powder was brought up in 500 μL of 50 mM $TbCl_3$ buffer (containing 10 mM Tris, 10 mM NaCl, 50 mM Tb_3Cl, 85 mM sodium citrate, pH 7.4) and freeze-thawed ten times (dry ice/50°C water bath). The sample was then passed through a 0.4 μm filter ten times and immediately buffer exchanged with DPA on a size exclusion column (Superdex 200 10/300, GE Healthcare, Sweden). Liposomes were then diluted to 2.5% (*v*/*v*) prior to use. 200 μL of the DPA-suspended Tb^{3+}-loaded liposomes were added to each well of a Corning flat bottom, black polystyrene 96-well plates (Sigma-Aldrich, USA). Appropriate concentrations of Lumacaftor were added to the wells and mixed well using a pipette. Plates were then covered and left for 1 hour at room temperature. Tb^{3+} fluorescence was measured using a SpectraMax i3X Multi-Mode Assay Microplate Reader (Molecular Devices, USA). Tb^{3+} was excited at 314 nm (bandwidth 9 nm), and the emission was recorded at 544 nm (bandwidth 15 nm), with 18 flashes per read. The temperature was kept constant at 25°C. Fluorescence was recorded for each well, and fluorescence of liposomes alone was subtracted from the samples with added drug. All samples were normalized to the fluorescence of a 0.1% Triton-lysed control.

SUPPORTING FIGURES

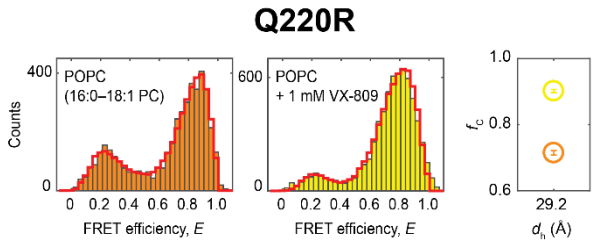

Figure S1. FRET efficiency histograms of Q220R in POPC vesicles in the absence of VX-809 (orange) and at 1 mM VX-809 (yellow), both determined at room temperature. PDA fits are shown as red cityscapes. Right panel: Fractions of closed hairpin (f_C) as function of hydrophobic thickness (d_h) as determined by PDA fits. Errors are standard deviations of the PDA chi-square minimization algorithm calculated from ten iterations.

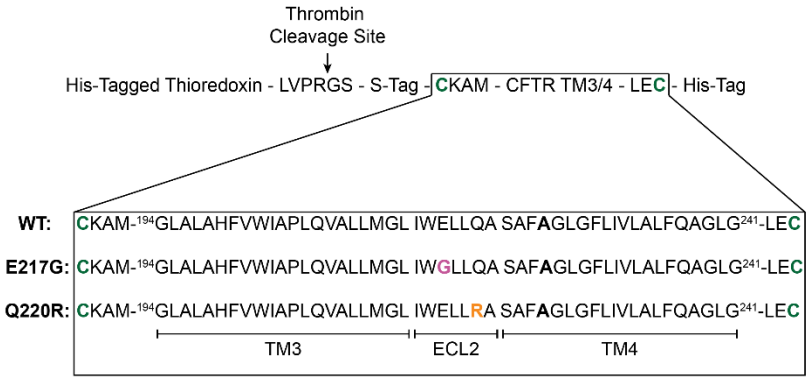

Figure S2. Design and amino acid sequence of WT, E217G, and Q220R TM3/4 hairpin fusion constructs. The locations of the two point mutations E217G and Q220R in ECL2 are highlighted in pink and orange, respectively. The two Cys residues used for labeling are indicated in green. The Ala residue at position 225 (indicated in bold) replaces a native Cys residue, so that unspecific fluorescent labeling of TM3/4 by thiol-maleimide chemistry was prevented.

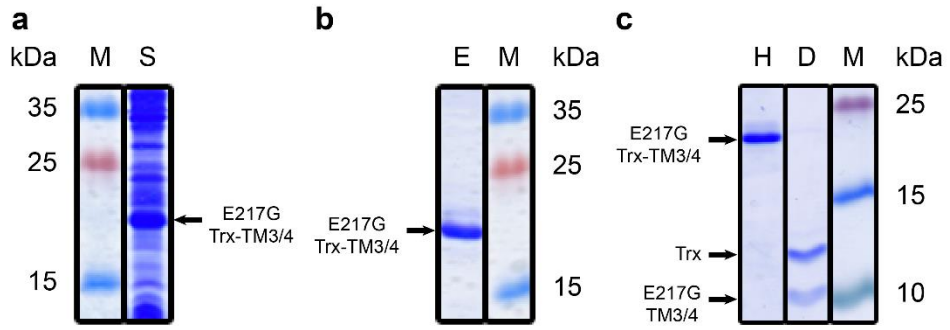

Figure S3. Purification of the E217G TM3/4 hairpin followed by SDS-PAGE. (a) Soluble fraction (S) after cell lysis and centrifugation. (b) Elution fraction (E) after purification by IMAC. (c) Sample after heat treatment (H) and after thrombin digestion (D). Bands for the Thioredoxin(Trx)–TM3/4 fusion protein (23.4 kDa), the cleaved E217G TM3/4 hairpin (9.4 kDa) and Trx tag (13.9 kDa) are indicated by an arrow. M, Molecular-weight protein marker (PageRuler Plus Prestained Protein Ladder, Thermo Fisher); the molecular weights are indicated (kDa). Samples were analyzed on 12% (a,b) and 16% (c) SDS-PAGE gels and stained with Coomassie Brilliant Blue.

SUPPORTING REFERENCES

1. Krainer, G., Treff, A., Hartmann, A., Stone, T. A., Schenkel, M., Keller, S., Deber, C. M., and Schlierf, M. (2018) A minimal helical-hairpin motif provides molecular-level insights into misfolding and pharmacological rescue of CFTR. *Commun. Biol.* **1**, 154
2. Krainer, G., Gracia, P., Frotscher, E., Hartmann, A., Gröger, P., Keller, S., and Schlierf, M. (2017) Slow Interconversion in a Heterogeneous Unfolded-State Ensemble of Outer-Membrane Phospholipase A. *Biophys. J.* **113**, 1280–1289
3. Hartmann, A., Krainer, G., Keller, S., and Schlierf, M. (2015) Quantification of Millisecond Protein-Folding Dynamics in Membrane-Mimetic Environments by Single-Molecule Förster Resonance Energy Transfer Spectroscopy. *Anal. Chem.* **87**, 11224–11232
4. Krainer, G., Hartmann, A., Anandamurugan, A., Gracia, P., Keller, S., and Schlierf, M. (2018) Ultrafast Protein Folding in Membrane-Mimetic Environments. *J. Mol. Biol.* **430**, 554–564